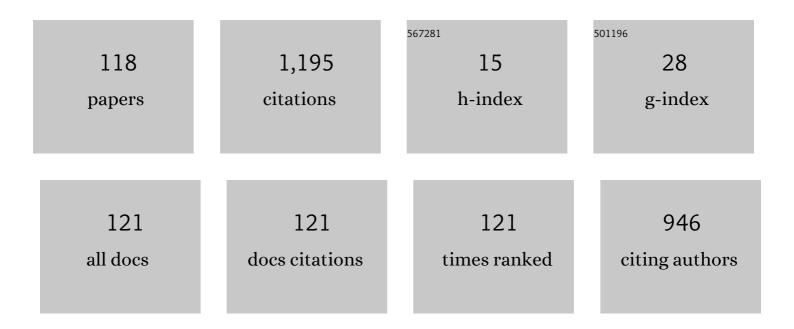
List of Publications by Year in descending order

Source: https://exaly.com/author-pdf/1559735/publications.pdf Version: 2024-02-01



SHIDO KUBURI

#	Article	IF	CITATIONS
1	Self-assembly of MoS2 nanosheet adhered on Fe-MOF heterocrystals for peroxymonosulfate activation via interfacial interaction. Journal of Colloid and Interface Science, 2022, 608, 3098-3110.	9.4	22
2	Development of electrically conductive ZrO2-CaO-Fe2O3-V2O5 glass and glass-ceramics as a new cathode active material for Na-ion batteries with high performance. Journal of Alloys and Compounds, 2022, 899, 163309.	5.5	4
3	Electrical Transport in Iron Phosphate-Based Glass-(Ceramics): Insights into the Role of B2O3 and HfO2 from Model-Free Scaling Procedures. Nanomaterials, 2022, 12, 639.	4.1	3
4	Elucidating the Mechanistic Origin of a Spin State-Dependent FeN <sub><i>x</i></sub> –C Catalyst toward Organic Contaminant Oxidation via Peroxymonosulfate Activation. Environmental Science & Technology, 2022, 56, 1321-1330.	10.0	81
5	Mössbauer study of some novel iron-bis-glyoxime and iron-tris-glyoxime complexes. Hyperfine Interactions, 2022, 243, 1.	0.5	2
6	Highly covalent FeIII–O bonding in photo-Fenton active Sn-doped goethite nanoparticles. Materials Chemistry and Physics, 2022, 287, 126247.	4.0	4
7	Structural, electrical and photocatalytic properties of iron-containing soda-lime aluminosilicate glass and glass-ceramics. Journal of Non-Crystalline Solids, 2021, 553, 120510.	3.1	13
8	Influence of Cr doping on the structural, magnetic, optical and photocatalytic properties of α-Fe2O3 nanorods. Journal of Physics and Chemistry of Solids, 2021, 148, 109699.	4.0	16
9	Photocatalytic degradation of organic dyes and phenol by iron-silicate glass prepared by the sol–gel method. New Journal of Chemistry, 2021, 45, 19019-19031.	2.8	8
10	Influence of low-spin Co3+ for high-spin Fe3+ substitution on the structural, magnetic, optical and catalytic properties of hematite (I±-Fe2O3) nanorods. Journal of Physics and Chemistry of Solids, 2021, 152, 109929.	4.0	12
11	Self-Assembly of Nanosheet-Supported Fe-MOF Heterocrystals as a Reusable Catalyst for Boosting Advanced Oxidation Performance via Radical and Nonradical Pathways. ACS Applied Materials & Interfaces, 2021, 13, 22694-22707.	8.0	40
12	Structural characterization, electrical and photocatalytic properties of αâ~and γ-Fe2O3 nanoparticles dispersed in iron aluminosilicate glass. Journal of Non-Crystalline Solids, 2021, 561, 120756.	3.1	12
13	Municipal waste slag for dyes photocatalytic and metal recovery applications through structural analysis and experimental characterization. International Journal of Energy Research, 2021, 45, 17691-17708.	4.5	4
14	BiOBr/MoS2 catalyst as heterogenous peroxymonosulfate activator toward organic pollutant removal: Energy band alignment and mechanism insight. Journal of Colloid and Interface Science, 2021, 594, 635-649.	9.4	51
15	Local structure, glass transition, structural relaxation, and crystallization of functional oxide glasses investigated by MA¶ssbauer spectroscopy and DTA. Journal of Materials Science: Materials in Electronics, 2021, 32, 23655-23689.	2.2	5
16	Structural characterization and visible light activated photocatalytic ability of glass–ceramics prepared from municipal solid waste. Journal of Material Cycles and Waste Management, 2021, 23, 2266-2277.	3.0	2
17	57Fe-Mössbauer and XAFS Studies of Conductive Sodium Phospho-Vanadate Glass as a Cathode Active Material for Na-ion Batteries with Large Capacity. Journal of Non-Crystalline Solids, 2021, 570, 120998.	3.1	9
18	Synthesis, characterization and magnetic properties of ε-Fe2O3 nanoparticles prepared by sol-gel method. Journal of Magnetism and Magnetic Materials, 2021, 538, 168264.	2.3	16

#	Article	IF	CITATIONS
19	Magnetic property and 57Fe Mössbauer analysis of dilute Fe and Nb codoped SrTiO3-δ(STO) perovskites. Hyperfine Interactions, 2020, 241, 1.	0.5	3
20	Photo-Fenton catalytic ability of iron-containing aluminosilicate glass prepared by sol-gel method. Journal of Alloys and Compounds, 2020, 816, 153227.	5.5	12
21	PVP surfactant-modified flower-like BiOBr with tunable bandgap structure for efficient photocatalytic decontamination of pollutants. Applied Surface Science, 2020, 530, 147233.	6.1	67
22	Structural characterization and magnetic properties of iron-phosphate glass prepared by sol-gel method. Journal of Non-Crystalline Solids, 2020, 543, 120158.	3.1	5
23	Emergence of ferromagnetism due to charge transfer in compressed ilmenite powder using super-high-energy ball milling. Scientific Reports, 2020, 10, 5293.	3.3	2
24	Photo-Fenton degradation of methylene blue using hematite-enriched slag under visible light. Journal of Radioanalytical and Nuclear Chemistry, 2020, 325, 537-549.	1.5	16
25	The relationship between local structure and photo-Fenton catalytic ability of glasses and glass-ceramics prepared from Japanese slag. Journal of Radioanalytical and Nuclear Chemistry, 2019, 322, 751-761.	1.5	9
26	Mössbauer and photocatalytic studies of CaFe2O4 nanoparticle-containing aluminosilicate prepared from domestic waste simulated slag. Journal of Radioanalytical and Nuclear Chemistry, 2019, 322, 1469-1476.	1.5	4
27	119Sn and 57Fe MÓ§ssbauer study of highly conductive vanadate glass. Journal of Materials Science: Materials in Electronics, 2019, 30, 8847-8854.	2.2	4
28	State analysis of fluorine-doped SnO2 (FTO) by 57Fe Mössbauer spectroscopy. Hyperfine Interactions, 2019, 240, 1.	0.5	0
29	Determination of iron species, including biomineralized jarosite, in the iron-hyperaccumulator moss Scopelophila ligulata by MA¶ssbauer, X-ray diffraction, and elemental analyses. BioMetals, 2019, 32, 171-184.	4.1	1
30	Influence of Fe(III) doping on the crystal structure and properties of hydrothermally prepared β-Ni(OH)2 nanostructures. Journal of Alloys and Compounds, 2018, 750, 687-695.	5.5	30
31	Improving the visible-light photocatalytic activity of SnOx·SiO2 glass systems by introducing SnOx nanoparticles. Journal of Radioanalytical and Nuclear Chemistry, 2018, 316, 579-586.	1.5	0
32	Structural relaxation and electrical conductivity of molybdovanadate glass. Journal of Materials Science: Materials in Electronics, 2018, 29, 2654-2659.	2.2	4
33	Effect of Substitutional Doping of Tin in Highly Conductive Barium Iron Vanadate Glass. Physica Status Solidi (A) Applications and Materials Science, 2018, 216, 1800157.	1.8	6
34	57Fe and 119Sn Mössbauer, XRD, FTIR and DC conductivity study of Li2O Fe2O3SnO2P2O5 glass and glass ceramics. Journal of Alloys and Compounds, 2018, 765, 121-127.	5.5	18
35	Effect of phosphorus precursors on the structure of bioactive calcium phosphate silicate systems. Materials Science and Engineering C, 2017, 73, 767-777.	7.3	6
36	The relationship between SnII fraction and visible light activated photocatalytic activity of SnOx·SiO2 glass studied by Mössbauer spectroscopy. Journal of Radioanalytical and Nuclear Chemistry, 2017, 311, 1859-1865.	1.5	3

#	Article	IF	CITATIONS
37	Waste water purification using new porous ceramics prepared by recycling waste glass and bamboo charcoal. Applied Water Science, 2017, 7, 4281-4286.	5.6	5
38	57Fe-Mössbauer study and methylene blue decomposing effect of nanoparticle mixtures composed of metallic iron and maghemite. Journal of Alloys and Compounds, 2017, 722, 94-100.	5.5	9
39	Highly conductive barium iron vanadate glass containing different metal oxides. Pure and Applied Chemistry, 2017, 89, 419-428.	1.9	10
40	Visible-light activated photocatalytic effect of glass and glass ceramic prepared by recycling waste slag with hematite. Pure and Applied Chemistry, 2017, 89, 535-544.	1.9	13
41	Synthesis and properties of indium-doped hematite. Journal of Alloys and Compounds, 2017, 695, 1900-1907.	5.5	27
42	Mössbauer study of pH dependence of iron-intercalation in montmorillonite. Hyperfine Interactions, 2016, 237, 1.	0.5	4
43	The effects of In 3+ doping on the properties of precipitated goethite. Journal of Alloys and Compounds, 2016, 658, 41-48.	5.5	11
44	A relationship between electrical conductivity and structural relaxation of 10SnO <sub>2</sub> ·10Fe <sub>2</sub> 0 <sub>3</sub> &m	iddot;10P	<sub>28</sub>
	heat-treatment. Journal of the Ceramic Society of Japan, 2015, 123, 121-128.		
45	B23-P-20The STEM Study of Crystalized Iron Vanadate Glasses Containing Alkaline Earth Oxide. Microscopy (Oxford, England), 2015, 64, i121.2-i121.	1.5	Ο
46	Synthesis of 14C labeled C60 with higher specific radioactivity. Journal of Radioanalytical and Nuclear Chemistry, 2015, 303, 1233-1237.	1.5	0
47	Photocatalytic effect and Mössbauer study of iron titanium silicate glass prepared by sol-gel method. Hyperfine Interactions, 2015, 232, 51-58.	0.5	3
48	Synthesis and microstructural properties of mixed iron–gallium oxides. Journal of Alloys and Compounds, 2015, 634, 130-141.	5.5	17
49	Structural Study of Glass and Glass Ceramics Prepared with Egyptian Basalt. Silicon, 2015, 7, 383-391.	3.3	16
50	Structural analysis and visible light-activated photocatalytic activity of iron-containing soda lime aluminosilicate glass. Journal of Alloys and Compounds, 2015, 645, 1-6.	5.5	11
51	The formation and microstructural properties of uniform $\hat{I}_{\pm}$ -GaOOH particles and their calcination products. Journal of Alloys and Compounds, 2015, 620, 217-227.	5.5	38
52	Characterization and Conduction Mechanism of Highly Conductive Vanadate Glass. Croatica Chemica Acta, 2015, 88, 427-435.	0.4	13
53	Role of Sulfur as a Reducing Agent for the Transition Metals Incorporated into Lithium Silicate Glass. Croatica Chemica Acta, 2015, 88, 505-510.	0.4	4
54	Structural Characterization of Electrical Conductive Vanadate Glass. Radioisotopes, 2014, 63, 117-117.	0.2	0

#	Article	IF	CITATIONS
55	Degradation of Trichloroethylene and Methylene Blue by a Mixture of Fe0 and γ-Fe2O3 â^ A Review. ACS Symposium Series, 2014, , 179-191.	0.5	1
56	$ ext{M} ilde{ extsf{q}}$ ssbauer study of conductive oxide glass. AIP Conference Proceedings, 2014, , .	0.4	4
57	Magnetic interaction in oxygenated alpha Fe-phthalocyanines. , 2014, , .		1
58	Mössbauer study of metallic iron and iron oxide nanoparticles having environmental purifying ability. , 2014, , .		3
59	Visible Light-Activated Photocatalytic Effect of Iron-Containing Silicate Glass - A Review. ACS Symposium Series, 2014, , 71-84.	0.5	1
60	57Fe-Mössbauer study of electrically conductive alkaline iron vanadate glasses. Journal of Radioanalytical and Nuclear Chemistry, 2014, 299, 453-459.	1.5	8
61	Visible light activated photo-catalytic effect and local structure of iron silicate glass prepared by sol-gel method. Hyperfine Interactions, 2014, 226, 747-753.	0.5	13
62	Electrical conductivity and local structure of lithium iron tungsten vanadate glass. Hyperfine Interactions, 2014, 226, 755-763.	0.5	0
63	Mössbauer study of novel iron(II)-dioxime complexes with branched alkyl chains. Hyperfine Interactions, 2014, 226, 181-185.	0.5	7
64	Controlled crystallization a ionic conductivity of nanostructured LiNbFePO 4 glass ceramic. Hyperfine Interactions, 2014, 226, 131-140.	0.5	2
65	Mössbauer study of new vanadate glass with large charge-discharge capacity. Hyperfine Interactions, 2014, 226, 765-770.	0.5	5
66	Local structure and water cleaning ability of iron oxide nanoparticles prepared by hydro-thermal reaction. Hyperfine Interactions, 2014, 226, 489-497.	0.5	1
67	Visible light activated catalytic effect of iron containing soda-lime silicate glass characterized by 57Fe-MA¶ssbauer spectroscopy. Journal of Radioanalytical and Nuclear Chemistry, 2014, 301, 1-7.	1.5	12
68	A relationship between oxidation state of iron and color of Arita celadon glaze characterized by <sup>57</sup> Fe-Mössbauer spectroscopy. Journal of the Ceramic Society of Japan, 2014, 122, 520-522.	1.1	6
69	Structural Characterization of Electrical Conductive Vanadate Glass. Radioisotopes, 2014, 63, 69-77.	0.2	0
70	Mössbauer study of FINEMET with different permeability. Hyperfine Interactions, 2013, 219, 63-67.	0.5	7
71	Electrical conductivity and local structure of lithium tin iron vanadate glass. Hyperfine Interactions, 2013, 219, 141-145.	0.5	6
72	Characterization of electrically conductive vanadate glass containing tungsten oxide. Journal of Radioanalytical and Nuclear Chemistry, 2013, 295, 1123-1128.	1.5	8

#	Article	IF	CITATIONS
73	Enhancement of electrical conductivity and chemical durability of 20R2O•10Fe2O3•xWO3•(70â^'x)V2O5 glass (R=Na, K) caused by structural relaxation. Journal of Non-Crystalline Solids, 2013, 378, 227-233.	3.1	12
74	Water cleaning ability and local structure of iron-containing soda-lime silicate glass. Hyperfine Interactions, 2013, 218, 41-45.	0.5	6
75	Decomposition mechanism of methylene blue caused by metallic iron-maghemite mixture. Hyperfine Interactions, 2013, 218, 47-52.	0.5	6
76	Various Three-Dimensional Structures Connected by Al–O/OH/Acetate–Al Bonds. Inorganic Chemistry, 2013, 52, 13238-13243.	4.0	8
77	Effect of the structural change of an iron–iron oxide mixture on the decomposition of trichloroethylene. Journal of Radioanalytical and Nuclear Chemistry, 2013, 295, 23-30.	1.5	6
78	[sup 57]Fe Mol̀^ssbauer study of conductive vanadate glass with high chemical durability. AIP Conference Proceedings, 2012, , .	0.4	1
79	[sup 57]Fe MoÌ^ssbauer study of iron-containing soda-lime silicate glass with COD reducing ability. , 2012, , .		2
80	Non-HPLC Rapid Separation of Metallofullerenes and Empty Cages with TiCl <sub>4</sub> Lewis Acid. Journal of the American Chemical Society, 2012, 134, 9762-9767.	13.7	70
81	Propriedades estruturais e eletrônicas de óxidos de ferro em esmaltes celadon (II). Ceramica, 2012, 58, 534-541.	0.8	4
82	Reclassification of CK chondrites confirmed by elemental analysis and Fe-Mössbauer spectroscopy. Hyperfine Interactions, 2012, 208, 75-78.	0.5	1
83	Electrical conductivity and local structure of barium manganese iron vanadate glass. Hyperfine Interactions, 2012, 207, 61-65.	0.5	11
84	Effect of nanocrystallization on the electrical conduction of silver lithium phosphate glasses containing iron and vanadium. Hyperfine Interactions, 2012, 205, 91-95.	0.5	0
85	Mechanically strengthened new Hagi porcelain developed by controlling the chemical environment of iron. Hyperfine Interactions, 2012, 211, 173-180.	0.5	1
86	M^ ^ouml;ssbauer Study of Water-Resistive Conductive Vanadate Glass. Radioisotopes, 2012, 61, 463-468.	0.2	15
87	Water cleaning ability and local structure of iron-containing soda-lime silicate glass. , 2012, , 197-201.		0
88	Decomposition mechanism of methylene blue caused by metallic iron-maghemite mixture. , 2012, , 203-208.		0
89	Electrical conductivity and local structure of lithium tin iron vanadate glass. , 2012, , 459-463.		0
90	Local structures and electronic band states of αâ^'Fe2O3 polycrystalline particles in the glazes of the HIZEN celadons produced in the Edo period of Japan, by means of X-ray absorption spectra (II). Ceramica, 2011, 57, 155-165.	0.8	2

#	Article	IF	CITATIONS
91	Mechanical strength and local structure of 'new' Hagi porcelain investigated by <sup>57</sup> Fe-MA¶ssbauer spectroscopy. Journal of Physics: Conference Series, 2010, 217, 012067.	0.4	1
92	Mössbauer study of oxygen adducts in solid Fe(II) phthalocyanines. Journal of Physics: Conference Series, 2010, 217, 012029.	0.4	3
93	Electrical conductivity and local structure of iron-containing lithium barium vanadate glass. Journal of Physics: Conference Series, 2010, 217, 012026.	0.4	3
94	Structural Characterization of Gel-Derived Calcium Silicate Systems. Journal of Physical Chemistry A, 2010, 114, 10403-10411.	2.5	87
95	Dissolution behaviour of iron silicate glass. Hyperfine Interactions, 2009, 192, 31-36.	0.5	2
96	Dissolution behaviour of iron silicate glass. , 2009, , 533-538.		0
97	57Fe-Mössbauer study of electrically conducting barium iron vanadate glass after heat treatment. Hyperfine Interactions, 2008, 185, 115-121.	0.5	0
98	Reduction of iron(III) in annealed asbestos/chrysotile. Hyperfine Interactions, 2008, 186, 161-166.	0.5	1
99	A Mossbauer Study of the Low Spin-High Spin Transition of an Oxygen Adduct Formed in Solid β -Fe(II)Phthalocyanine. Open Inorganic Chemistry Journal, 2008, 2, 69-72.	0.3	2
100	Crystallization and Structural Relaxation of xBaO (90-x)V2O5 10Fe2O3 Glasses Accompanying an Enhancement of the Elctric Conductivity. Journal of the Ceramic Society of Japan, 2007, 115, 776-779.	1.1	23
101	Incorporation of Fe in the interlayer of Na-bentonite <i>via</i> treatment with FeCl <sub>3</sub> in acetone. Clays and Clay Minerals, 2007, 55, 89-95.	1.3	11
102	Corelationship between local structure and water purifying ability of iron-containing waste glasses. Hyperfine Interactions, 2006, 166, 429-436.	0.5	6
103	Effect of FeCl3 and acetone on the structure of Na–montmorillonite studied by Mössbauer and XRD measurements. Hyperfine Interactions, 2006, 166, 643-649.	0.5	5
104	Corelationship between local structure and water purifying ability of iron-containing waste glasses. , 2006, , 429-436.		2
105	Mössbauer study of semiconducting and ferrimagnetic fly ash-recycled glass. Journal of Radioanalytical and Nuclear Chemistry, 2005, 266, 171-177.	1.5	11
106	'Ea-δrule' applied to the crystallization study of gallate and vanadate glasses. Journal of Radioanalytical and Nuclear Chemistry, 2005, 266, 527-532.	1.5	0
107	Solidification of Hazardous Heavy Metal Ions with Soda-Lime Glass. Characterization of Iron and Zinc in the Waste Glass Journal of the Ceramic Society of Japan, 2000, 108, 245-248.	1.3	15
108	Title is missing!. Journal of Radioanalytical and Nuclear Chemistry, 2000, 246, 43-49.	1.5	4

#	Article	IF	CITATIONS
109	Title is missing!. Journal of Radioanalytical and Nuclear Chemistry, 2000, 246, 51-56.	1.5	2
110	Application of the "Tg-Δ rule―to the local structural study of ferrate glasses. Journal of Radioanalytical and Nuclear Chemistry, 1999, 239, 237-240.	1.5	7
111	Mössbauer study on the crystallization of IR-transmitting aluminate glasses. Journal of Radioanalytical and Nuclear Chemistry, 1999, 239, 303-307.	1.5	5
112	'TgDELTA. Rule' Applied to Semiconducting Vanadate Glasses Containing Different Amounts of Fe2O3 Journal of the Ceramic Society of Japan, 1999, 107, 408-412.	1.3	7
113	Substitution of Fe(III) for Ga(III) in calcium gallate glass confirmed from the Debye temperature. Journal of Radioanalytical and Nuclear Chemistry, 1998, 237, 47-50.	1.5	2
114	Crystallization mechanism of aluminoferrate glass accompanying a precipitation of nanocrystals of dicalcium ferrite (Ca2Fe2O5) and mayenite (12CaO·7Al2O3). Journal of Materials Chemistry, 1997, 7, 1801-1806.	6.7	29
115	Application of the IR transmission method and the Mössbauer effect to the crystallization of calcium gallate glass. Journal of Non-Crystalline Solids, 1997, 209, 87-95.	3.1	5
116	Occupation of tungsten site by iron in sodium tungstate glasses. Journal of Non-Crystalline Solids, 1996, 194, 23-33.	3.1	30
117	Laser- and gamma-ray induced crystallization of IR-transmitting calcium gallate glass. Hyperfine Interactions, 1994, 94, 2125-2130.	0.5	2
118	IR transmission method applied to the crystallization of gallate glasses and the mechanism of crystallization caused by Ar+ laser and 60Co Î <sup>3</sup> -ray irradiation. Journal of Non-Crystalline Solids, 1994, 177, 193-199.	3.1	11